Journal of Agricultural Sciences (Tarim Bilimleri Dergisi) 2024, 30 (2) : 386 – 399 DOI: 10.15832/ankutbd.1380604

Journal of Agricultural Sciences
(Tarim Bilimleri Dergisi)

J Agr Sci-Tarim Bili
e-ISSN: 2148-9297
jas.ankara.edu.tr

Rapid synthesis of Silver Nanoparticles with *Rheum ribes* L Fruit Peels: Anticancer and Antimicrobial Effects with Biocompatible Structures

Murat ZOR[a], Mehmet Fırat BARAN[b*], Duygu Neval SAYIN İPEK[c]

[a]*Department of Pharmacognosy, Faculty of Pharmacy, Fenerbahçe University, Ataşehir, İstanbul, TURKEY*

[b]*Vocational School of Technical Sciences, Food Technology Program, Batman University, TURKEY*

[c]*Dicle University, Faculty of Veterinary Medicine, Department of Pre-Clinical Sciences, Department of Veterinary Parasitology, Diyarbakir, TURKEY*

ARTICLE INFO
Research Article
Corresponding Author: Mehmet Fırat BARAN, E-mail: mfiratbaran@gmail.com
Received: 24 October 2023 / Revised: 04 December 2023 / Accepted: 11 December 2023 / Online: 26 March 2024

Cite this article
Zor M, Baran M F, Sayın İpek D N (2024). Rapid synthesis of Silver Nanoparticles with *Rheum ribes* L Fruit Peels: Anticancer and Antimicrobial Effects with Biocompatible Structures. *Journal of Agricultural Sciences (Tarim Bilimleri Dergisi),* 30(2):386-399. DOI: 10.15832/ankutbd.1380604

ABSTRACT
Silver nanoparticles (AgNPs) are substances with a wide range of uses. Utilizing extracts obtained from the peels of *Rheum ribes* L. (Rr) fruit growing in Erzurum region, silver nanoparticles were rapidly created in this study with a quick, easy, and environmentally friendly technique without harmful processes. In order to evaluate the attributes of the synthesized Rr-AgNPs, FE-SEM or TEM micrographs were utilized to characterize their morphology. A UV-visible spectrophotometer was used to assess the highest absorbance bands of RR-AgNPs. These data were used to define RR-AgNPs, which were characterized as having exclusively negative surface charges of -25 mV, spherical shape, maximum absorbance at 428 nm wavelength, and 96 nm size distribution. The effectiveness of the produced AgNPs for use in medical applications was assessed using the MTT technique with microdilution. Minimum inhibition concentrations of Rr-AgNPs for pathogen strains ranged from 0.03 to 0.50 mg/L. Additionally, it was discovered that AgNPs effectively suppressed malignant cells, with rates of 86.27%, 74.67%, and 73.49%, in the investigation of the anticancer effects of AgNPs. Healthy cells were not subject to any inhibitory effects at the same concentrations.

Keywords: Rr-AgNPs, Fruit peels, FTIR, TGA, UV-Vis

1. Introduction

Among the nanosciences, green nanotechnology is one of the most interesting areas with widespread areas of use producing and controlling elements at the molecular level (SI et al. 2020). Nanoparticles (NPs) are used in both scientific study and industrial applications, and they are crucial to both (J. Singh et al. 2018). The range of use of nanoparticles is quite wide. They are products with superior physical properties such as surface area, as well as chemically important properties (Kumar et al. 2017; Baran 2019a). Metallic nanoparticles such as zinc (Zn), palladium (Pd), gold (Au), and silver (Ag) are commonly used (Ismail et al. 2017; Baran 2019; Pandiyan et al. 2019; Baran et al. 2021).

AgNPs have uses in medical applications as antimicrobial, antioxidant, anticancer and anti-inflammatory agents. In addition, AgNPs are valuable particles in many areas such as bioremediation applications, the food industry, catalysis studies, and cosmetics (Velmurugan et al. 2014; Francis et al. 2017; V. Kumar et al. 2017; 2019; Thomas et al. 2018 Mohammadi et al. 2019; Abu-Dief et al. 2020; Arroyo et al. 2020). It is possible to obtain these valuable products using various methods. Among these methods, green synthesis methods, which are among biologically-sourced synthesis methods, have various advantages over physical, chemical, and other biologically-sourced environmentally friendly methods. Some of these advantages include being economical with low cost, no toxic chemicals used in synthesis, easy process, not requiring special conditions, and high yield of product obtained as a result of the synthesis (Al-ogaidi et al. 2017; Patil et al. 2018b; Rolim et al. 2019).

AgNPs are used in medical applications as antimicrobial and anticancer agents. Their use as an antimicrobial agent can contribute to the search for a solution to antibiotic resistance, which is a very important global problem in today's world (Kumar et al. 2017; A. Singh et al. 2018; Oliveira et al. 2019; Azmi et al. 2021). A terrible disease that has been studied extensively in the search for a cure is cancer. In addition to traditional approaches, studies about different treatment processes have attracted a great deal of attention. As a result, numerous studies have been conducted about the use of Rr-AgNPs as anticancer agents (Remya et al. 2015; Chung et al. 2016; Sarkar et al. 2018; Satpathy et al. 2018; Abu-Dief et al. 2020; Zein et al. 2020).

Rheum ribes L. (Rr), known as "Işgın" or "Kurdish banana", is a species belonging to the Polygonaceae family. This perennial herbaceous plant grows in the Iran-Turan floristic region. It is naturally found in rocky areas in regions such as Erzurum, Hakkari, Bingöl and Elazığ in Eastern Anatolia in Turkey. The length of its shoots can reach approximately 40 cm. The plant is beneficial against ulcers, diabetes, obesity, hypertension and digestive problems. It is frequently consumed as food for these reasons. In addition, the plant forms the raw material for many medicines in the Middle East. The plant contains significant amounts of phytochemical components such as phenolic acid and flavonoids. These phytochemicals have antimicrobial, anticancer and antioxidant bioactivities (Munzuroğlu 2000; Tosun & Kizilay 2003; Naqishbandi et al. 2009; Çınar Ayan et al. 2020).

This study used an extract from the fruit peel of Rr cultivated in Erzurum to create Rr-AgNPs by bioreduction and evaluated their antibacterial and anticancer activities in medical applications.

2. Material and Methods

2.1. Materials

Rr fruit was collected in Erzurum Çat district on May 2, 2022. The species was identified by Dr. Kenan Akbaş at Muğla Sıtkı Koçman University, Department of Biology Herbarium and was given Herbarium number K.A 1658-A.

2.1.1. Preparation of extract from fruit peels and silver nitrate solution

Fruit peels were removed and rinsed with distilled water before being dried. Dried fruit peels were weighed to 20 g and placed in a 500 mL beaker. Then 250 mL of distilled water was added and the mixture was heated until boiling. After being filtered with filter paper and brought to room temperature, the extract was ready for synthesis. A solution with a concentration of 5 mM was prepared from Sigma-Aldrich silver nitrate ($AgNO_3$) salt to be used to obtain Rh-AgNPs by bioreduction.

2.2. Methods

2.2.1. Bioreduction synthesis of Rr-AgNPs with fruit peel extract

For this, 200 mL of fruit peel extract and 200 mL of 5 mM $AgNO_3$ solution were combined 1:1 in a 1000 mL glass Erlenmeyer and left to sit at room temperature. The color shift was observed. By obtaining samples from the reaction medium at different times and performing UV-vis wavelength scans, along with color change, the presence of AgNPs at maximum absorbance was identified (Baran et al. et al. 2021; Atalar et al. 2022).

2.2.2. Characteristics of the produced Rr-AgNPs

To exhibit the formation of AgNPs synthesized from *R. ribes* fruit peel extract (Rh-AgNPs), samples were taken from this medium, with reaction-related color change after mixing the extract with $AgNO_3$ solution, and a Perkin Elmer One UV visible spectrophotometer was used (UV-vis). Maximum absorbances were measured in the 300-800 nm wavelength range. Using Fourier transformation infrared spectroscopy (FTIR-Perkin Elmer), frequency changes in the range of 4000-800 cm^{-1} for both the extract and the liquid obtained at the end of the reaction were examined to evaluate bioactive functional groups in the extract responsible for bioreduction. The morphological appearance of the synthesized Rh-AgNPs was evaluated in micrographs taken using Jeol Jem FE-SEM and TEM devices. In addition, topographic structures, shape, and size distributions of Rh-AgNPs were determined by means of AFM. Also, the size distribution was determined using Marven DLS. Graphs obtained using a RadB-DMAX II computer-controlled electron dispersed X-ray (EDX) were examined, and the elemental contents of the synthesized particles were determined. Plane-reflected crystal patterns were identified for Rh-AgNPs in data acquired at 2θ using a Rigaku Miniflex 600 model X-ray diffraction (XRD). With this data, crystal nanosizes were calculated using the Debye-Scherrer equation via XRD data (Baran & Acay 2019; Umaz et al. 2019). The charge distributions of the surface structures of the synthesized Rh-AgNPs were evaluated with Marven Zeta potential. The resistance of Rh-AgNPs to temperature changes was measured between 25 and 900 ℃ using Shimadzu 50 thermogravimetric and differential thermal analysis (TGA-DTA).

2.2.3. Antimicrobial Effects of Rh-AgNPs

Minimum inhibition concentrations (MIC) of Rh-AgNPs synthesized with fruit peel extract were calculated using the microdilution method (Atalar et al. 2022) for suppression of the growth of microorganisms in pathogenic groups. Pathogenic gram-negative and positive bacteria and yeast were used in the experimental study. Each microorganism was grown in suitable media for 24-48 hours of incubation at 37 °C. Then, microorganisms were prepared according to McFarland standard 0.5 (Emmanuel et al. 2015; Patil et al. 2021; Raghavendra et al. 2022) turbidity criteria for each strain. Bacteria and fungi were transferred to 96-well microplates containing the appropriate medium. Some wells on the microplate were selected and defined for the control groups. Then, Rh-AgNPs prepared at different concentrations were transferred to the microplate wells and microdilution was applied. The microorganisms were then transferred to the wells. The prepared microplates allowed interaction between microorganisms and Rh-AgNPs for 24-48 hours in an oven at 37 °C. At the end of the period, growth control was performed and MIC values were determined. İnönü University Medical Faculty Hospital Microbiology Laboratory provided the strains of *Staphylococcus aureus* (*S. aureus*) ATCC 25923, *Escherichia coli* (*E. coli*) ATCC 25922, and *Candida albicans* (*C. albicans*) ATCC 10231. Artuklu University Microbiology Research Laboratory provided the strains of *Bacillus subtilis* (*B. subtilis*) ATCC 11774 and *Pseudomonas aeruginosa* (*P. aeruginosa*) ATCC 27853.

2.2.4. Anticancer effects of Rh-AgNPs

Cytotoxic effects of the synthesized Rh-AgNPs on cancer cells were evaluated by determining the % survival rate using the MTT method (Baran et al. 2021). Three different cancer cells and one healthy cell were used in experimental studies. The cells were incubated in suitable nutrient media and under optimum conditions. Cells were then suspended at different concentrations using a hemocytometer, transferred to 96-well microplates, and incubated for 24 hours. Then, solutions containing Rh-AgNPs at different concentrations were added to the wells cultured with cell lines and incubated for 48 hours. The absorbance of the cells was then read using a Multi Scan Go (Thermo) instrument at 540 nm. The viability suppressing concentrations of Rh-AgNPs in the cell lines were calculated with the following formula (Remya et al. 2015; Mohmed et al. 2017; Sunderam et al. 2019; Chen et al. 2021).

$$\text{Viability \%} = (\text{sample absorbance} / \text{control absorbance}) \times 100 \quad (2)$$

3. Results and Discussion

3.1. Maximum absorbance bands obtained via UV-vis data of Rh-AgNPs

A color change from yellow to brown was observed 35 minutes after combining Rr fruit peel extract with $AgNO_3$ solution, which is a macroscopic finding indicating that Rh-AgNPs had formed (Acay and Baran, 2019; Jebril et al. 2020; Mamdooh & Naeem, 2021; Mani et al. 2021; Sattari et al. 2021). In addition to this finding, the maximum absorbance bands at 428 nm taken with UV-vis were characteristic, showing the vibrations (SPR) occurring on the plasma surface and the formation and presence of Rh-AgNPs (Figure 1) (Luna et al. 2015; Patra et al. 2016; Francis et al. 2017; Eren & Baran 2019; Anandalakshmi 2021).

In a study in which AgNPs were synthesized using the fruit of the Rh plant and 1 mM $AgNO_3$ solution in a ratio of 10:1, respectively, the maximum wavelength absorbance of the obtained AgNPs was 425 nm (Mustafa, Mahdi Auda, Hajir, Ali Shareef & Bari 2021). In this study, the maximum absorbance of AgNPs obtained by using the fruit peels of the Rh plant and 5 mM $AgNO_3$ solution in a 1:1 ratio was 428 nm. UV-vis findings of the studies show that the maximum wavelengths were almost the same, despite the use of different parts of the plant, different extracts and metal concentrations. In another study using Rh fruit, the maximum wavelength absorbance of AgNPs obtained using the ethanol extract in an medium with 10 mM $AgNO_3$ concentration at 200 rpm at 75 ℃ for two days was 410 nm (Aygün et al. 2020). This study is more advantageous in terms of application conditions such as the method of obtaining the extract, synthesis temperature, shaking and metal concentration.

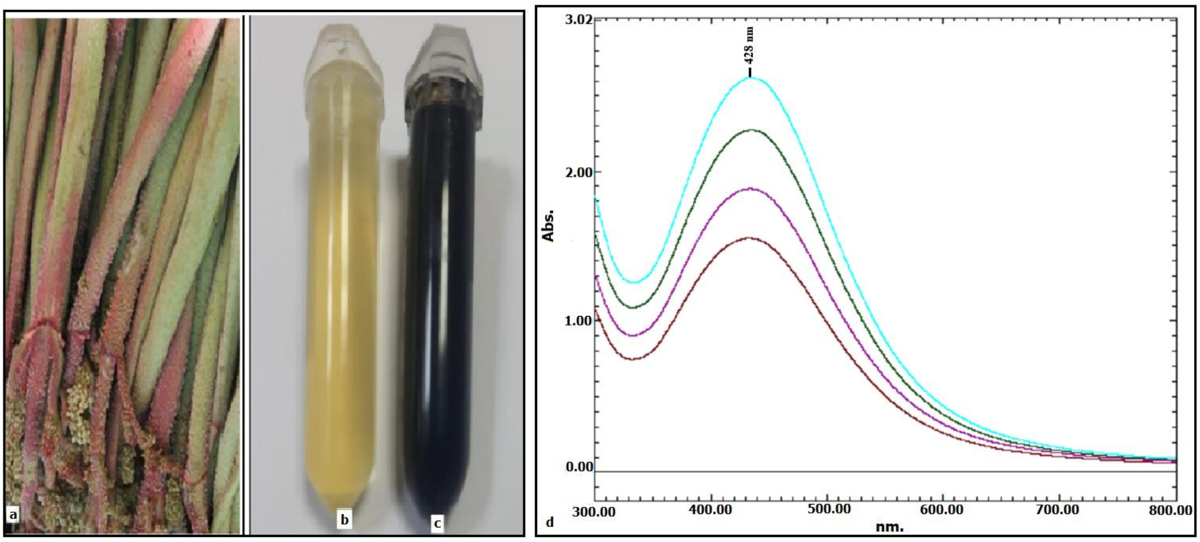

Figure 1- a. Rr fruit b. Rr fruit extract, c. The appearance of the end-reaction fluid indicates the formation of Rr-AgNPs as a result of synthesis, and d. Maximum absorbance spectra dependent on SPR according to UV-vis for the presence of Rr-AgNPs

3.2. XRD Analysis of Rr-AgNPs

In Figure 2, data obtained at 2θ with XRD was evaluated to calculate the crystal patterns and nanosizes of Rr-AgNPs. Widening of the Bragg angle peaks showed that the Rh-AgNPs have a central faceted cubic pattern (fcc) (A. Singh et al. 2018; Wongpreecha et al. 2018a; 2018b; Jebril et al. 2020; Anandalakshmi 2021). The FWHM values of 111º, 200º, 220º, and 311º Bragg angles in the data were determined as 38.72, 44.62, 64.90, and 77.48, respectively. By using Debye-Sherrer's high peak FWHM value for the crystal nano dimensions of Rr-AgNPs, the cubic pattern of Rr-AgNPs was calculated to have crystal size of 58.06 nm. In two green synthesis studies using Rh fruits, the crystal patterns of the obtained AgNPs had similar characteristics with broadening peaks occurring at 111º, 200º, 220º, and 311º Bragg angles (Aygün et al. 2020; Mustafa et al. 2021). In the biosynthesis study of AgNPs using *Cucurbita maxima* L. extracts, the crystal nanosizes of AgNPs were calculated as 67 and 56 nm (Ali 2020). In studies using herbal extracts for the synthesis of AgNPs, the crystal nanosizes were calculated as 24.36 nm (Khan et al. 2022), 40 nm, and 21.17 nm (Aktepe & Baran 2021).

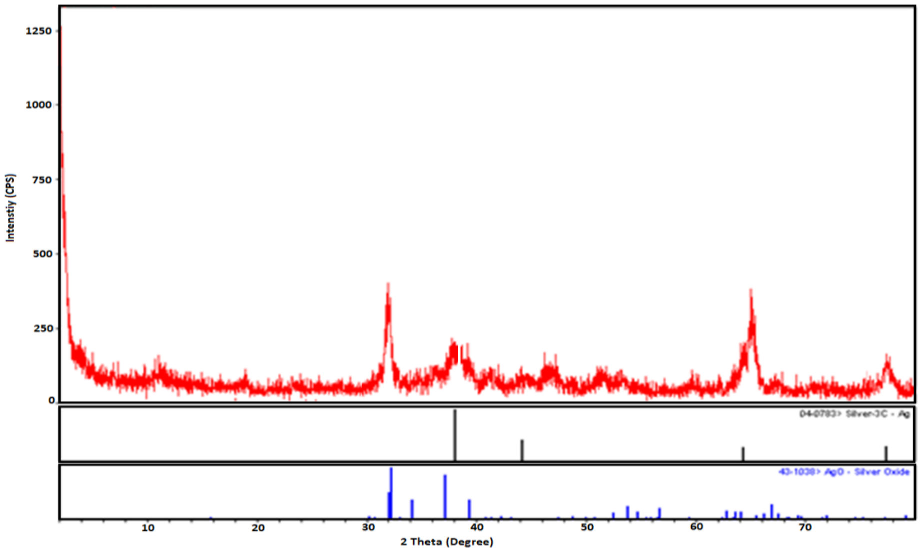

Figure 2- Data from X-ray diffraction showing the crystal structures of Rr-AgNPs.

3.3. FTIR Spectroscopy Data

The FTIR spectra of the liquid media as a result of extract synthesis were analyzed in order to assess the groups of bioactive substances that may control bioreduction and stability. Frequency changes in the data occur at 3337.81-3330 cm^{-1}. In order to assess the groups of bioactive components ensuring bioreduction, stability of Ag^{+} form to Ag^{o} form, and the stability of produced nanoparticles were investigated from 2122.95-2122.80 cm^{-1}, and 1635.48-1635.33 cm^{-1}. These observations demonstrated the potential for aromatic chains with C=C stretching, flavonoid-phenolic groups with C=O stretching, and hydroxyl groups resulting from O-H stretching to affect bioreduction and durability (Figure 3) (B. Kumar et al. 2015; Ahmad et al. 2018; A. U. Khan et al. 2018; Hemmati et al. 2019; Jogaiah et al. 2019; Jebril et al. 2020;Auda et al. 2021).

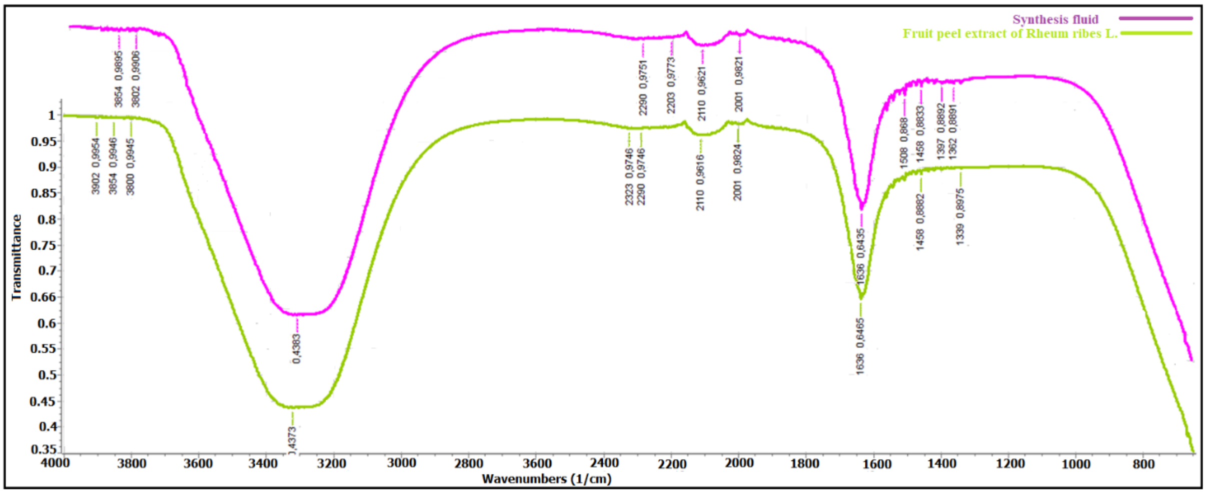

Figure 3- FTIR spectra of Rr fruit peel extract and reaction liquid obtained after synthesis

3.4. SEM and EDX Images of Rr-AgNPs

In SEM micrographs, the synthesized Rr-AgNPs had spherical morphology (Figure 4). According to reports, Rr-AgNPs had spherical morphology in SEM images taken during green synthesis investigations (Satpathy et al. 2018; Jebril et al. 2020; Aktepe & Baran 2021).

The profile of the EDX graph was used to determine the elemental contents of the particles synthesized with fruit peel extract (Figure 5). Strong peaks in the areas for elemental silver indicated that the synthesized particles were Rr-AgNPs (Pallela et al. 2018; Butola et al. 2019; M. R. Khan et al. 2022; Suriyakala et al. 2022). The existence of phytochemicals that actively contribute to the stability of the medium around Rr-AgNPs was suggested by weak peaks for elements in the graph, such as carbon and oxygen (Vastrad 2016; Kumar et al. 2019; Das et al. 2021). FTIR and zeta potential results in Figures 3 and 7, respectively, further confirm this data.

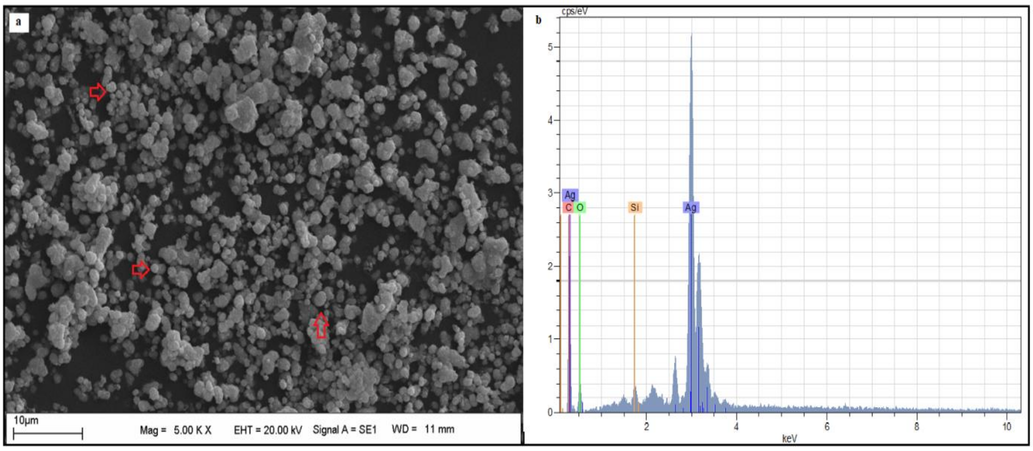

Figure 4- Rr-AgNPs after synthesis with Rr fruit peel extract; a. SEM micrograph of morphology and b. EDX profile

3.5. Appearance of Rr-AgNPs in FESEM and TEM Micrographs

Figure 5 shows images taken with a FESEM and TEM microscope of Rr-AgNPs produced with Rr fruit peel extract. The figure shows that the synthesized Rh-AgNPs exhibited spherical morphological appearance. AgNPs had the same morphological appearance in both studies using Rh fruit (Aygün et al. 2020; Auda et al. 2021). AgNPs synthesized in other green synthesis studies using different plant sources had the same morphological appearance (Velmurugan et al. 2014; Remya et al. 2015; Mamdooh & Naeem 2021; Wang et al. 2021).

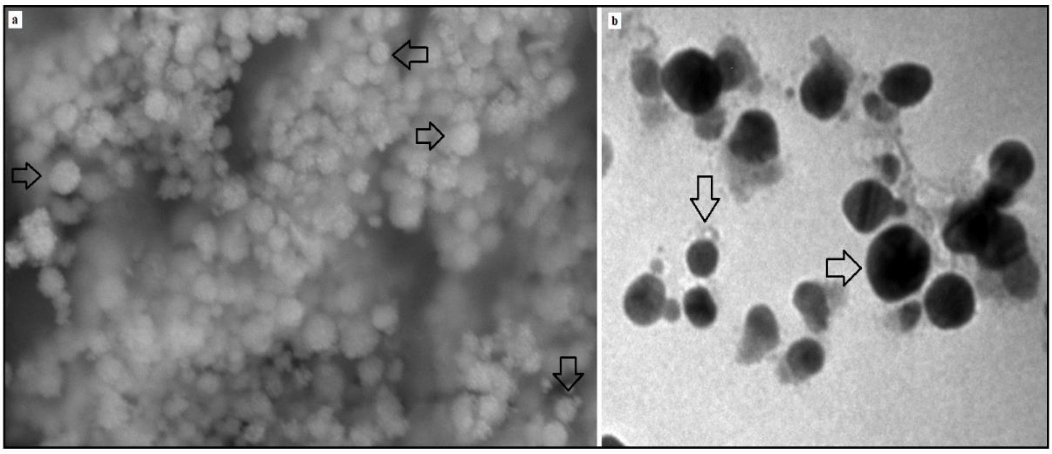

Figure 5- Rr-AgNPs after synthesis with Rr fruit peel extract; a. FE-SEM ve b. TEM micrograph of morphological views

3.6. TGA-DTA analysis of synthesized Rr-AgNPs

The thermal resistance of the synthesized Rr-AgNPs was determined by TGA-DTA analysis data at 10-800 °C. In the data, there were 5.98%, 8.24%, 23.73%, and 15.17% mass losses, respectively, occurring at 27.35-158.88 °C, 159.99-289.13 °C, 291.71-458.03 °C, and 458.03-801.53 °C (Figure 5). The loss of water absorbed was the cause of the initial mass loss (7.07%). The presence of flavonoids surrounding the surface of Rr-AgNPs caused mass losses at the other three temperatures (Baran 2019b; Rolim et al. 2019; Baran et al. 2021). The weak C, O peaks and -25 mV negative surface charge in the EDX and Zeta potential data in Figures 5 and 7, respectively, also support this finding.

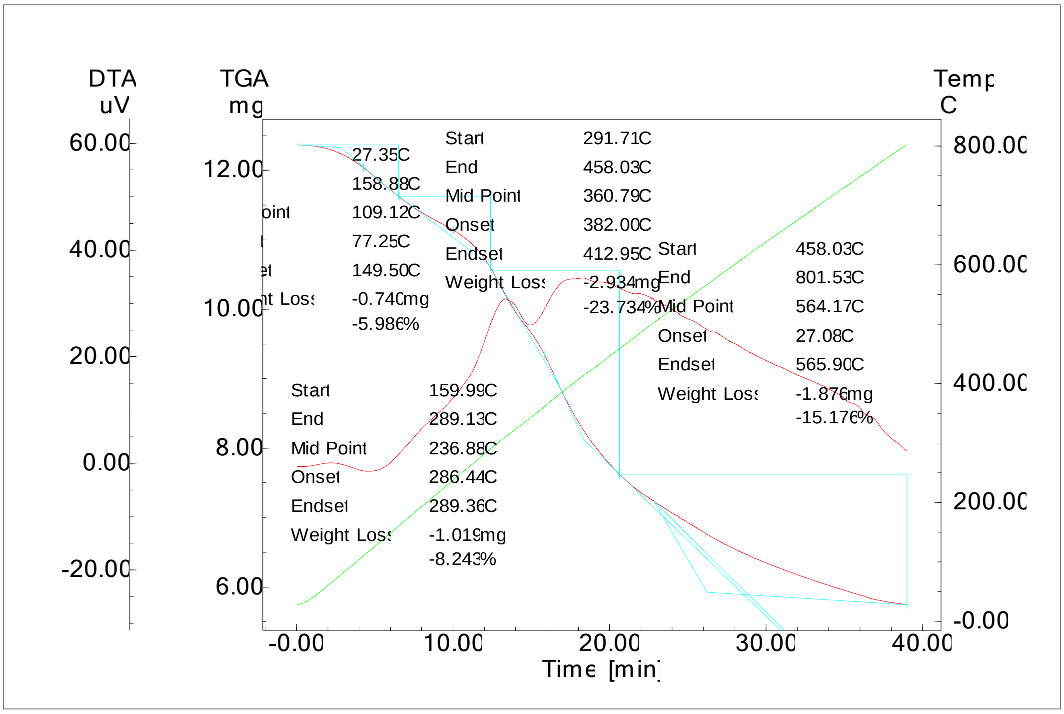

Figure 6- TGA-DTA data for Rr-AgNPs with mass loss points against heat treatment

3.7. Zeta potential analyses of synthesized Rr-AgNPs

The surface charges of Rr-AgNPs synthesized using fruit peel extract were identified as -25 mV by zeta potential analysis (Figure 7). The negative charge distribution of Rr-AgNPs is an important indicator of their stability. Green synthesized Rr-AgNPs exhibit more efficient negative charge distribution compared to those obtained by other synthesis approaches. The existence of flavonoids in the surface structure of Rr-AgNPs influences the distribution of negative charges. A negative charge arrangement stabilizes free electrons in colloidal form by oxidizing the hydroxyl groups. (Pugazhendhi et al. 2018; Wongpreecha et al. 2018b; Oliveira et al. 2019; Jebril et al. 2020; Aktepe et al. 2022). The presence of phytochemicals around Rr-AgNPs in the findings obtained in Figure 3, Figure 5, and Figure 6 also contribute to the explanation for the surface structure. The fact that the surface charges of the synthesized Rr-AgNPs have different charges (negative and positive) triggers the formation of negative results that affect stability, such as fluctuation and aggregation, as the nanoparticles attract with each other by electrostatic attraction (Al-ogaidi et al. 2017; Patil et al. 2018a; Satpathy et al. 2018). The -25 mV surface charge data showed that the synthesized Rr-AgNPs were stable. It was reported that Rr-AgNPs synthesized from different plant sources had surface charge distribution of 25.01 mV (Aktepe et al. 2022), −22 ± 5 mV (Ferreyra Maillard et al. 2018), and -19 mV (Oliveira et al. 2019).

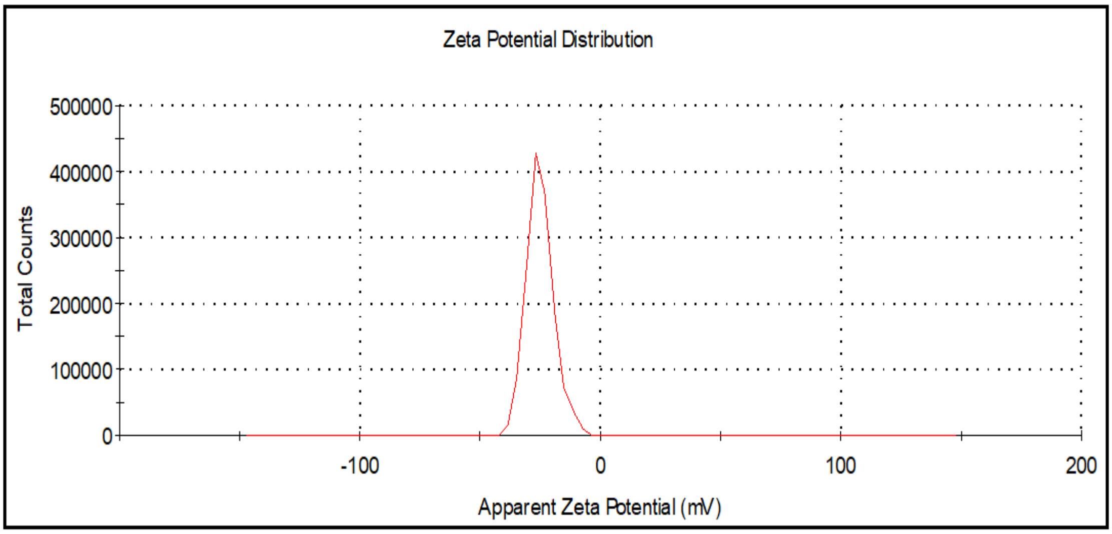

Figure 7- Graphs of zeta potential charge distribution of Rr-AgNPs after synthesis

3.8. Density-dependent Rr-AgNPs size distribution

The mean size distribution of the produced Rh-AgNPs, as seen in Figure 8, is 96 nm. They had an average size distribution of 54 nm in a study about the manufacture of AgNPs utilizing extracts from *Crinum asiaticum* leaves (Shukla et al. 2022). According to Kumar et al. (2017), AgNPs made with *Prunus persica* extract had size distribution of 2-130 nm. According to reports from earlier studies about environmentally friendly synthesis, the produced AgNPs had size distribution between 59.74 nm and 268 nm (Alkhulaifi et al. 2020; Mamdooh & Naeem 2021).

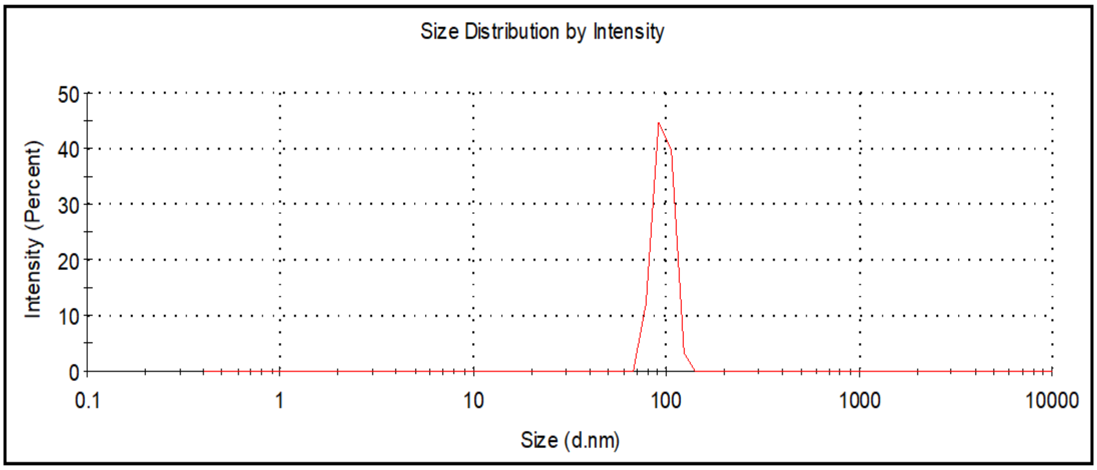

Figure 8- Density-dependent size distribution of synthesized Rr-AgNPs

3.9. AFM Micrograph of the distributions of synthesized Rr-AgNPs

As shown in Figure 9, the topographical features and morphologies of the produced Rr-AgNPs were determined by analyzing AFM data. The data showed that Rr-AgNPs were less than 100 nm, exhibited spherical appearance, and were distributed in a single structure (Swamy et al. 2015; Kumar et al. 2017; Rauf et al. 2021).

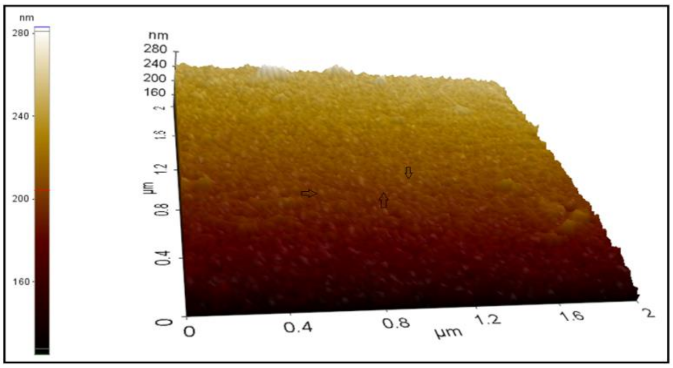

Figure 9- AFM micrograph of Rr-AgNPs synthesized using fruit peel extract

3.10. Antimicrobial effects of synthesized Rr-AgNPs

By using the microdilution method, the MIC values of the produced Rr-AgNPs for the development of pathogenic microbes were examined. In Table 1 and Figure 9, the MIC values affecting the growth of the strains are given. As seen in the data, 0.03-0.50 µmg/L concentrations had a suppressive effect on growth of microorganisms. The effective MIC values of the synthesized Rr-AgNPs were 0.03-0.13 and 0.25-0.50 mg/L for gram positive and negative bacteria, respectively. These values were considerably lower than the effective concentrations of silver nitrate solution and antibiotics. The effective MIC value for the fungus *C. albicans* was found to be 0.03 µmg/L, and this value is also many times lower than the value at which silver nitrate solution and antibiotics were effective. Table 2 gives the MIC values of Rr-AgNPs obtained in some applications using green synthesis.

Rr-AgNPs ionize in liquid media and show high reactivity. They approach one other with the electrical force of attraction, interacting with organisms in the exact same environment (Narayan & Dipak 2015; Ahmed et al. 2016; Chung et al. 2016; Zhang, et al. 2010; Aina et al. 2018). They cause defects in the membrane structure of microorganisms and adversely affect the functions of DNA, RNA, and vital enzymes, which have high affinity for these species due to the increase in reactive oxygen species (ROS). The structure of the biomolecules is damaged by these species and as a result, their functions deteriorate and the microorganism dies (Emmanuel et al. 2015; Shao et al. 2018; Huq et al. 2022).

Table 1- MIC values for Rh-AgNPs, antibiotics and silver nitrate solution with antimicrobial effect on the growth of microorganisms

Microorganisms		***AgNPs µg/mL***	***Silver Nitrate µg/mL***	***Antibiotic µg/mL***
Gram Positive	*B. subtilis* ATCC 11774	0.13	2.65	2.00
	S. aureus ATCC 29213	0.03	1.32	1.00
Gram Negative	*E. coli* ATCC25922	0.25	0.66	2.00
	P. aeruginosa ATCC27833	0.50	1.32	4.00
Fungus (Yeast)	*C. albicans* ATCC 10231	0.03	0.66	2.00

Commercial antibiotics used: **vancomycin** for gram (+) bacteria, **colistin** for gram (-) bacteria, and **fluconazole** for *C. albicans*.

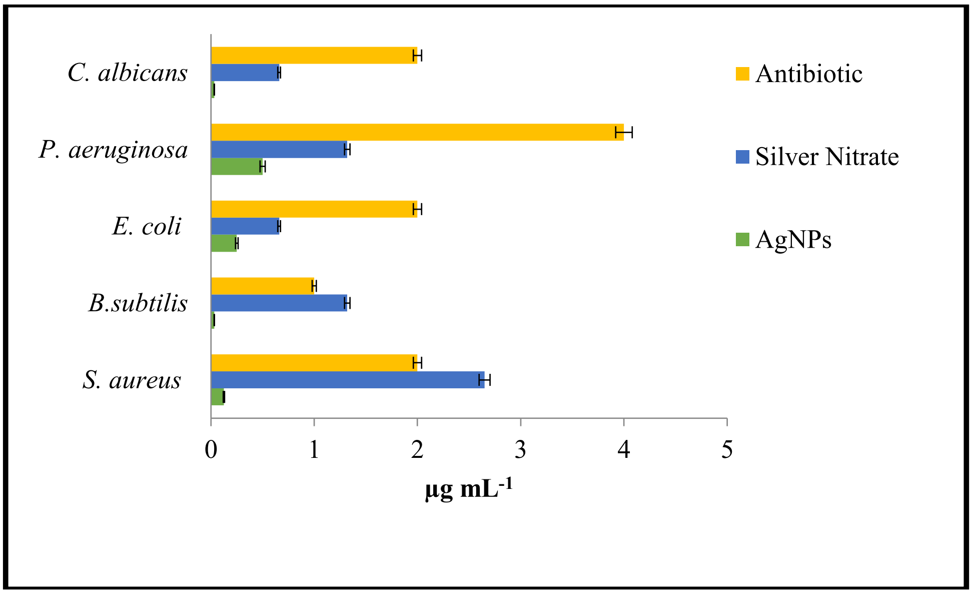

Figure 9- Graph of MIC values of Rh-AgNPs, $AgNO_3$ solution, and antibiotics Commercial antibiotics used: vancomycin for gram (+) bacteria, colistin for gram (-) bacteria, and fluconazole for *C. albicans*.

Table 2- Antimicrobial effects of AgNPs obtained in green synthesis studies

Biological Source	***Size (nm)***	***Gram Negative µg/mL***	***Gram Positive µg/mL***	***References***
Agastache foeniculum	9-19	12.50	6.25	(Polivanova et al. 2021)
Vitis vinifera	18.53	0.31	0.07	(Acay et al. 2019)
Fritillaria sp.	10	1-2	1-4	(Hemmati et al. 2019)
Zataria multiflora	25	1.25	0.5-4	(Barabadi et al. 2021)
Euphorbia hirta	15.5	0.67	0.82	(V. Kumar et al. 2016)
Madhuca longifolia	30-50	80-90	40-60	(Patil et al. 2018b)

3.11. Anti-cancer effects of Rr-AgNPs

The MTT technique was used to investigate the viability-suppressing concentrations of Rr-AgNPs made using Rr fruit peel for healthy cell lines and the suppressive effects for cancer cell lines. Up to a concentration of 25-200 mg/L, the Rr-AgNPs were not hazardous for the normal cell line HDF. However, it had a very strong suppressive impact on lines of cancer cells, indicating a very positive outcome for use as an anticancer drug. Even at a 25 mg/L dosage, a good suppressive effect was seen. With an inhibitory rate of 86.27%, 74.67%, and 73.49% for U118, CaCo-2, and Skov-3, 100 mg/L concentration was discovered to have excellent anticancer effect (Table 3 and Figure 10). Due to the existence of extensive vascular holes in the target cancer cells, the tiny size of NPs impacts the build-up and penetration of NPs into these areas. Additionally, Rr-AgNPs have a propensity to accumulate in crucial components such as membranes of cells, proteins, and nuclei. After localization, Rr-AgNPs with strong oxidative characteristics cause the cell to die by inducing cell death mechanisms such apoptosis and an increase in ROS As a result of these impacts, it is crucial to assess the harmful effects of Ag+ ions in living organisms (Wongpreecha et al. 2018b). Some NP characteristics contribute to harmful impacts.

Table 3- Viability percentages after Rr-AgNP interactions with various cell lines using the MTT technique for 48 hours.

Cell Line	***25 µmg/L***	***50 µmg/L***	***100 µmg/L***	***200 µmg/L***
HDF	79.45	67.55	67.55	41.00
U118	64.82	58.71	13.73	8.68
CaCo-2	23.74	23.08	26.51	34.11
Skov-3	86.18	73.77	25.33	32.22

HDF; human skin fibroblast cells: **U118**; glioblastoma cells: **CaCo-2**; colon cancer cells: **Skov-3**; ovarian sarcoma cells

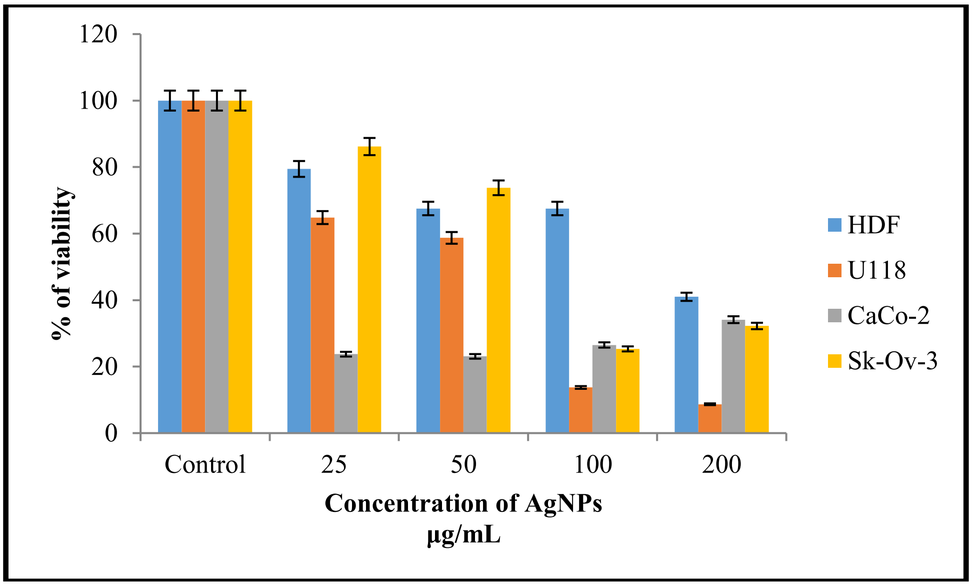

Figure 10- Viability percentages after Rr-AgNP interactions with various cell lines using the MTT technique for 48 hours.In Table 4, the cytotoxic effects on cancer cells of some nanoparticles obtained with green synthesis are compared.

Table 4- Amounts of Rr-AgNPs found in research employing environmentally friendly synthesis methods that contribute to the cytotoxic impact

Biological Source	***Cancer Cell Line***	***Size (nm)***	***Shape***	***Effective Concentration µmg/L***	***Refereces***
Aloe Vera	HDF	20	Spherical	100	(Zhang, et al. 2010)
Aspergillus sp.	CaCo-2	5-30	Spherical	3.75-5	(Mohmed et al. 2017)
Pueraria tuberosa	Skov-3	162.72	Spherical	29.36	(Satpathy et al. 2018)

4. Conclusions

Rr-AgNPs are widely used, which makes them very valuable materials. The manufacture of these items receives a lot of attention daily for green synthesis techniques. The extract from the peel of the Rr fruit, also known as "Işgin" or "Kurdish banana," which grows in the Erzurum region, was used in this study to produce Rr-AgNPs for the first time in a quick, straightforward, ecologically benign method without harmful processes. Data from TEM, AFM, UV-vis, FE-SEM, XRD, EDX, TGA-DTA, Zetasizer, and Zeta potential analyses were used to identify the characteristics of the synthesized Rr-AgNPs. In order to evaluate the functional components of flavonoids that contribute to bioreduction during the manufacturing process, FTIR data were examined. Maximum absorbance, spherical shape, median size range of 96 nm, and charge on the surface of -25 mV at wavelength of 428 nm were all characteristics of the produced Rr-AgNPs. The efficacy of produced Rr-AgNPs in medicinal applications was studied using MTT and microdilution techniques. The minimum inhibitory concentrations of Rr-AgNPs needed to inhibit hospital pathogens were between 0.03-0.50 mg/L. These concentrations were extremely low compared to antibiotics and $AgNO_3$ solution. With inhibitory rates of 86.27%, 74.67%, and 73.49%, Rr-AgNPs were discovered to have a very good anticancer impact on U118, CaCo-2, and Skov-3 cancer cells. The healthy cell HDF was not damaged by the same concentration. In particular for biopharmacology, enhancing application processes will considerably advance the search for antibacterial and anticancer drugs.

Declarations

Conflict of interest

All authors declare there are no conflicts of interest in this research work.

Acknowledgements

We would like to thank Dr Kenan Akbaş who identified the *Rheum ribes* L. plant.

References

Abu-Dief A M, Abdel-Rahman L H, Abd-El Sayed M A, Zikry M M & Nafady A (2020). Green Synthesis of AgNPs Ultilizing *Delonix Regia*

Extract as Anticancer and Antimicrobial Agents. ChemistrySelect 5: 13263–13268. https://doi.org/10.1002/slct.202003218
Acay H & Baran M F (2019). Biosynthesis and characterization of silver nanoparticles using king oyster (*Pleurotus eryngii*) extract: Effect on some microorganisms. Applied Ecology and Environmental Research 17:9205–9214. https://doi.org/10.15666/aeer/1704_92059214.
Acay H, Baran M F & Eren A (2019). Investigating Antimicrobial Activity of Silver Nanoparticles Produced Through Green Synthesis Using Leaf Extract of Common Grape (*Vitis Vinifera*) 17: 4539–4546
Ahmad T, Bustam M A, Irfan M, Moniruzzaman M, Anwaar Asghar H M & Bhattacharjee S (2018). Green synthesis of stabilized spherical shaped gold nanoparticles using novel aqueous *Elaeis guineensis* (oil palm) leaves extract. Journal of Molecular Structure 1159: 167–173. https://doi.org/10.1016/j.molstruc.2017.11.095
Ahmed K B A, Raman T &Veerappan A (2016) Future prospects of antibacterial metal nanoparticles as enzyme inhibitor. Materials Science and Engineering C 68:939–947. https://doi.org/10.1016/j.msec.2016.06.034.
Aina A D, Owolo O, Adeoye-Isijola M, Aina F O, Favour O &Adewumi A G (2018) Almond leaves for the one-pot Biofabrication of silver nanoparticles: Characterization and larvicidal application. International Journal of Scientific and Research Publications (IJSRP) 8:703–711. https://doi.org/10.29322/ijsrp.8.11.2018.p8378.
Aktepe & Baran A (2021) Biosynthesis of AgNPs by extract from waste leaves of *Citrullus lanatus* sp. (watermelon); characterization, antibacterial and antifungal effects. Department of Applied Mathematics and Statistics 23:e2021243. https://doi.org/10.23751/pn.v23i3.11907.
Aktepe N, Butuner H, Baran A, Baran M F & Keskin C (2022) Synthesis, characterization and evaluation of antimicrobial activities of silver nanoparticles obtained from *Rumex acetosella* L.(Sorrel) plant. International Journal of Agriculture Environment and Food Sciences. 6: 522-529. https://doi.org/10.31015/jaefs.2022.4.4.
Al-ogaidi I, Salman MI, Mohammad FI, Aguilar Z, Al- M, Hadi YA & Al-rhman RMA (2017) Antibacterial and Cytotoxicity of Silver Nanoparticles Synthesized in Green and *Black Tea*. World Journal of Experimental Biosciences 5:39–45.
Ali MH (2020) Eco-friendly synthesis of silver nanoparticles from crust of Cucurbita Maxima L. (red pumpkin). EurAsian Journal of BioSciences Eurasia J Biosci 14:2829–2833.
Anandalakshmi K (2021) Green synthesis, characterization and antibacterial activity of silver nanoparticles using chenopodium *album* leaf extract. Indian Journal of Pure and Applied Physics 59:456–461.
Arroyo G V, Madrid A T, Gavilanes A F, Naranjo B, Debut A, Arias MT& Angulo Y (2020) Green synthesis of silver nanoparticles for application in cosmetics. Journal of Environmental Science and Health - Part A Toxic/Hazardous Substances and Environmental Engineering 55:1304–1320. https://doi.org/10.1080/10934529.2020.1790953.
Atalar M N, Baran A, Hatipoğlu A, Baran M F, Yavuz Ö, Aktepe N & Keskin C. (2022) The Characterization of Silver Nanoparticles Synthesized From *Prunus spinosa* Fruit and Determination of Antimicrobial Effects on Some Food Pathogens. European Journal of Science and Technology 298–305. https://doi.org/10.31590/ejosat.1040082.
Auda M M., Shareef H A & Mohammed B L (2021). Green synthesis of Silver Nanoparticles using the extract of *Rheum ribes* and evaluating their antifungal activity against some of Candida sp. Tikrit Journal of Pure Science, 26(2), 53-59. https://doi.org/10.25130/tjps.v26i2.119
Aygun A, Gulbağça F, Nas M S, Alma M H, Çalımlı M H, Ustaoglu B &, Şen F (2020). Biological synthesis of silver nanoparticles using *Rheum ribes* and evaluation of their anticarcinogenic and antimicrobial potential: A novel approach in phytonanotechnology. Journal of pharmaceutical and biomedical analysis, 179:113012. doi:10.1016/j.jpba.2019.113012
Azmi SNH, Al-Jassasi BMH, Al-Sawafi HMS, Al-Shukaili SHG, Rahman N & Nasir M (2021) Optimization for synthesis of silver nanoparticles through response surface methodology using leaf extract of *Boswellia sacra* and its application in antimicrobial activity. Environmental Monitoring and Assessment 193:497. https://doi.org/10.1007/s10661-021-09301-w.
Barabadi H, Mojab F, Vahidi H, Marashi B, Talank N, Hosseini O & Saravanan M (2021) Green synthesis, characterization, antibacterial and biofilm inhibitory activity of silver nanoparticles compared to commercial silver nanoparticles. Inorganic Chemistry Communications 129:108647. https://doi.org/10.1016/j.inoche.2021.108647.
Baran M (2019) Synthesis of silver nanoparticles (AgNP) with *Prunus avium* cherry leaf extract and investigation of its antimicrobial effect. Dicle University Journal of Engineering 10:221–227. https://doi.org/10.24012/dumf.487255.
Baran M F. (2019a) Evaluation of Green Synthesis and Anti-Microbial Activities of AgNPs Using Leaf Extract of Hawthorn Plant. Research and Evaluations in Science and Mathematics 2019:110–120.(Book Chapter)
Baran M F. (2019b) Synthesis, Characterization and Investigation of Antimicrobials Activity Of Sılver Nanopartıcles From *Cydonia oblonga* Leaf. 17:2583–2592. https://doi.org/10.15666/aeer/1702_25832592.
Baran M F & Acay H (2019) Antimicrobial Activity of Silver Nanoparticles Synthesized with Extract of Tomato plant Against Bacterial and Fungal Pathogens. Middle Black Sea Journal of Health Science 67–73. https://doi.org/10.19127/mbsjohs.551132.Baran MF., Keskin C., Atalar M N., Baran A (2021) Environmentally Friendly Rapid Synthesis of Gold Nanoparticles from Artemisia absinthium Plant Extract and Application of Antimicrobial Activities. Journal of the Institute of Science and Technology 11:365–375. https://doi.org/10.21597/jist.779169.
Butola B S, Gupta A & Roy A (2019) Multifunctional finishing of cellulosic fabric via facile, rapid *in-situ* green synthesis of AgNPs using pomegranate peel extract biomolecules. Sustainable Chemistry and Pharmacy 12:100135. https://doi.org/10.1016/j.scp.2019.100135.
Chen J, Li Y, Fang G, Cao Z, Shang Y, Alfarraj S & Li J (2021) Green synthesis, characterization, cytotoxicity, antioxidant, and anti-human ovarian cancer activities of *Curcumae kwangsiensis* leaf aqueous extract green-synthesized gold nanoparticles. Arabian Journal of Chemistry 14:103000. https://doi.org/10.1016/j.arabjc.2021.103000.
Chung IM, Park I, Seung-Hyun K, Thiruvengadam M & Rajakumar G (2016) Plant-Mediated Synthesis of Silver Nanoparticles: Their Characteristic Properties and Therapeutic Applications. Nanoscale Research Letters 11:1–14. https://doi.org/10.1186/s11671-016-1257-4.
Çınar A İ, Çetinkaya S, Dursun H G & Suntar İ (2020) Bioactive Compounds of *Rheum ribes* L. and its Anticancerogenic Effect via Induction of Apoptosis and miR-200 Family Expression in Human Colorectal Cancer Cells. Nutrition and Cancer 73:1228–1243. https://doi.org/10.1080/01635581.2020.1792947.
Das G, Shin H, Kumar A & Vishnuprasad CN (2021) Photo-mediated optimized synthesis of silver nanoparticles using the extracts of outer shell fibre of *Cocos nucifera* L. fruit and detection of its antioxidant, cytotoxicity and antibacterial potential. *Saudi Journal of Biological Sciences* 28:980–987. https://doi.org/10.1016/j.sjbs.2020.11.022.
Emmanuel R, Palanisamy S, Chen S, Chelladurai K, Padmavathy S, Saravanan M, Al-hemaid & Fahad MA (2015) Antimicrobial efficacy of green synthesized drug blended silver nanoparticles against dental caries and periodontal disease causing microorganisms. Materials Science & Engineering C 56:374–379. https://doi.org/10.1016/j.msec.2015.06.033.

Eren, A & Baran M F (2019) Green Synthesis, Characterization and Antimicrobial Activity Of Silver Nanoparticles (AgNPs) From Maize (*Zea mays* L.). Applıed Ecology and Envıronmental Research 17:4097–4105. https://doi.org/10.15666/aeer/1702_40974105.

Ferreyra Maillard APV, Dalmasso PR, López de Mishima BA& Hollmann A (2018) Interaction of green silver nanoparticles with model membranes: possible role in the antibacterial activity. Colloids and Surfaces B: Biointerfaces 171:320–326. https://doi.org/10.1016/j.colsurfb.2018.07.044.

Francis S, Joseph S, Koshy EP & Mathew B (2017) Green synthesis and characterization of gold and silver nanoparticles using *Mussaenda glabrata* leaf extract and their environmental applications to dye degradation. Environmental Science and Pollution Research 24:17347–17357. https://doi.org/10.1007/s11356-017-9329-2.

Hemmati S, Rashtiani A, Zangeneh MM, Mohammadi P, Zangeneh A & Veisi H (2019) Green synthesis and characterization of silver nanoparticles using *Fritillaria* flower extract and their antibacterial activity against some human pathogens. Polyhedron 158:8–14. https://doi.org/10.1016/j.poly.2018.10.049.

Huq MA, Ashrafudoulla M, Rahman MM., Balusamy SR & Akter S (2022) Green Synthesis and Potential Antibacterial Applications of Bioactive Silver Nanoparticles: A Review. Polymers 14:1–22. https://doi.org/10.3390/polym14040742.

Ismail E, Khenfouch M, Dhlamini M, Dube S &Maaza M (2017) Green palladium and palladium oxide nanoparticles synthesized via *Aspalathus linearis* natural extract. Journal of Alloys and Compounds 695:3632–3638. https://doi.org/10.1016/j.jallcom.2016.11.390.

Jebril S, Khanfir Ben Jenana R & Dridi C (2020) Green synthesis of silver nanoparticles using *Melia azedarach* leaf extract and their antifungal activities: In vitro and in vivo. Materials Chemistry and Physics 248:122898. https://doi.org/10.1016/j.matchemphys.2020.122898.

Jogaiah S, Kurjogi M, Abdelrahman M., Hanumanthappa N & Tran LSP (2019) *Ganoderma applanatum*-mediated green synthesis of silver nanoparticles: Structural characterization, and *in vitro* and *in vivo* biomedical and agrochemical properties. Arabian Journal of Chemistry 12:1108–1120. https://doi.org/10.1016/j.arabjc.2017.12.002.

Khan A U, Yuan Q, Khan ZUH, Ahmad A, Khan FU, Tahir K & Ullah S (2018) An eco-benign synthesis of AgNPs using aqueous extract of *Longan* fruit peel: Antiproliferative response against human breast cancer cell line MCF-7, antioxidant and photocatalytic deprivation of methylene blue. *Journal of Photochemistry and Photobiology B: Biology* 183:367–373. https://doi.org/10.1016/j.jphotobiol.2018.05.007.

Khan MR, Hoque SM, Hossain KFB, Siddique MAB, Uddin MK & Rahman MM (2022) Green synthesis of silver nanoparticles using *Hibiscus sabdariffa* leaf extract and its cytotoxicity assay. Inorganic and Nano-Metal Chemistry 0:1–11. https://doi.org/10.1080/24701556.2021.2025091.

Kumar, R, Ghoshal, G. Jain A & GM (2017) Rapid Green Synthesis of Silver Nanoparticles (AgNPs) Using (*Prunus persica*) Plants extract: Exploring its Antimicrobial and Catalytic Activities. Journal of Nanomedicine & Nanotechnology 8:1–8. https://doi.org/10.4172/2157-7439.1000452.

Kumar B, Smita K, Cumbal L & Debut A (2015) Green synthesis of silver nanoparticles using *Andean blackberry* fruit extract. Saudi Journal of Biological Sciences 24:45–50. https://doi.org/10.1016/j.sjbs.2015.09.006.

Kumar V, Gundampati R K, Singh D K, Bano D, Jagannadham M V & Hasan S H (2016) Photoinduced green synthesis of silver nanoparticles with highly effective antibacterial and hydrogen peroxide sensing properties. Journal of Photochemistry and Photobiology B: Biology 162:374–385. https://doi.org/10.1016/j.jphotobiol.2016.06.037.

Kumar V, Singh DK, Mohan S, Gundampati RK & Hasan SH (2017) Photoinduced green synthesis of silver nanoparticles using aqueous extract of *Physalis angulata* and its antibacterial and antioxidant activity. Journal of Environmental Chemical Engineering 5:744–756. https://doi.org/10.1016/j.jece.2016.12.055.

Kumar V, Singh S, Srivastava B & Bhadouria R (2019) Journal of Environmental Chemical Engineering Green synthesis of silver nanoparticles using leaf extract of *Holoptelea integrifolia* and preliminary investigation of its antioxidant, anti- infl ammatory , antidiabetic and antibacterial activities. Journal of Environmental Chemical Engineering 7:103094. https://doi.org/10.1016/j.jece.2019.103094.

Luna C, Chávez VHG, Barriga-castro ED, Nú NO & Mendoza-reséndez R (2015) Biosynthesis of Silver Fine Particles and Particles Decorated with Nanoparticles Using the Extract of *Illicium Verum* (*Star Anise*) Seeds. Spectrochımıca Acta Part A: Molecular and Bıomolecular Spectroscopy 141:45–50. https://doi.org/10.1016/j.saa.2014.12.076.

Mamdooh NW &Naeem GA (2021) Green Synthesis, Characterization and Biological Activity of Silver Nanoparticles Using *Ruta* Leaf Extract. Journal of Physics: Conference Series 1999:1487–1499. https://doi.org/10.1088/1742-6596/1999/1/012050.

Mani M, Harikrishnan R, Purushothaman P, Pavithra S, Rajkumar P, Kumaresan S &Kaviyarasu K (2021) Systematic green synthesis of silver oxide nanoparticles for antimicrobial activity. Environmental Research 202:111627. https://doi.org/10.1016/j.envres.2021.111627.

Mohammadi F, Yousefi M & Ghahremanzadeh R (2019) Green Synthesis, Characterization and Antimicrobial Activity of Silver Nanoparticles (AgNps) Using Leaves and Stems Extract of Some Plants. Advanced Journal of Chemistry-Section A 2:266–275. https://doi.org/10.33945/SAMI/AJCA.2019.4.1.

Mohmed A, Hassan S, Fouda A, Elgamal M & Salem S (2017) Extracellular Biosynthesis of Silver Nanoparticles Using *Aspergillus sp*. and Evaluation of their Antibacterial and Cytotoxicity. Journal of Applied Life Sciences International 11:1–12. https://doi.org/10.9734/jalsi/2017/33491.

Munzuroglu O (2000) A Study of the Levels of Vitamins A, E and C and Selenium in *Rhubarb* (*Rheum ribes* L.). Turkish Journal of Biology 24:397–404.

Naqishbandi AM, Josefsen K, Pedersen ME & Jger AK (2009) Hypoglycemic activity of Iraqi *Rheum ribes* root extract. Pharmaceutical Biology 47:380–383. https://doi.org/10.1080/13880200902748478.

Narayan S & Dipak S (2015) Green synthesis of silver nanoparticles using fresh water green alga *Pithophora oedogonia* (Mont.) Wittrock and evaluation of their antibacterial activity. Applied Nanoscience 5:703–709. https://doi.org/10.1007/s13204-014-0366-6.

Oliveira A C de J, Araújo AR de, Quelemes PV, Nadvorny D, Soares-Sobrinho JL, Leite JRS de A & Silva DA da (2019) Solvent-free production of phthalated cashew gum for green synthesis of antimicrobial silver nanoparticles. Carbohydrate Polymers 213:176–183. https://doi.org/10.1016/j.carbpol.2019.02.033.

Pallela PNVK, Ummey S, Ruddaraju LK, Pammi SVN &Yoon SG (2018) Ultra Small, mono dispersed green synthesized silver nanoparticles using aqueous extract of *Sida cordifolia* plant and investigation of antibacterial activity. Microbial Pathogenesis 124:63–69. https://doi.org/10.1016/j.micpath.2018.08.026.

Pandiyan N, Murugesan B, Arumugam M, Sonamuthu J, Samayanan S & Mahalingam S (2019) Ionic liquid - A greener templating agent with *Justicia adhatoda* plant extract assisted green synthesis of morphologically improved Ag-Au/ZnO nanostructure and it's antibacterial and anticancer activities. Journal of Photochemistry and Photobiology B: Biology 198:111559. https://doi.org/10.1016/j.jphotobiol.2019.111559.

Patil MP, Seong YA, Kim JO, Seo YB & Kim G Do (2021) Synthesis of silver nanoparticles using aqueous extract of *Cuscuta japonica* seeds and their antibacterial and antioxidant activities. Inorganic Chemistry Communications 134:109035. https://doi.org/10.1016/j.inoche.2021.109035.

Patil M P, Singh R D, Koli P B, Patil K T, Jagdale B S, Tipare A R & Kim G (2018) Antibacterial potential of silver nanoparticles synthesized using *Madhuca longifolia* flower extract as a green resource. Microbial Pathogenesis 121:184–189. https://doi.org/10.1016/j.micpath.2018.05.040.

Patra J K, Das G & Baek K H (2016) Phyto-mediated biosynthesis of silver nanoparticles using the rind extract of watermelon (*Citrullus lanatus*) under photo-catalyzed condition and investigation of its antibacterial, anticandidal and antioxidant efficacy. Journal of Photochemistry and Photobiology B: Biology 161:200–210. https://doi.org/10.1016/j.jphotobiol.2016.05.021.

Polivanova O B, Cherednichenko M Y, Kalashnikova E A & Kirakosyan RN (2021) In vitro antibacterial effect of silver nanoparticles synthetized using Agastache foeniculum plant and callus extracts. AIMS Agriculture and Food 6:631–643. https://doi.org/10.3934/AGRFOOD.2021037.

Pugazhendhi S, Palanisamy P K & Jayavel R (2018) Synthesis of highly stable silver nanoparticles through a novel green method using *Mirabillis jalapa* for antibacterial, nonlinear optical applications. Optical Materials 79:457–463. https://doi.org/10.1016/j.optmat.2018.04.017.

Raghavendra VB, Shankar S, Govindappa M, Pugazhendhi A, Sharma M & Nayaka SC (2022) Green Synthesis of Zinc Oxide Nanoparticles (ZnO NPs) for Effective Degradation of Dye, Polyethylene and Antibacterial Performance in Waste Water Treatment. Journal of Inorganic and Organometallic Polymers and Materials 32:614–630. https://doi.org/10.1007/s10904-021-02142-7.

Rauf A, Ahmad T, Khan A, Maryam, Uddin G, Ahmad B &Al-Harrasi A (2021) Green synthesis and biomedicinal applications of silver and gold nanoparticles functionalized with methanolic extract of *Mentha longifolia*. Artificial Cells, Nanomedicine and Biotechnology 49:194–203. https://doi.org/10.1080/21691401.2021.1890099.

Remya RR, Rajasree SRR, Aranganathan L &Suman TY (2015) An investigation on cytotoxic effect of bioactive AgNPs synthesized using *Cassia fistula* flower extract on breast cancer cell MCF-7. Biotechnology Reports 8:110–115. https://doi.org/10.1016/j.btre.2015.10.004.

Rolim W R, Pelegrino M T, de Araújo Lima B, Ferraz L S, Costa F N, Bernardes J S &Seabra AB (2019) Green tea extract mediated biogenic synthesis of silver nanoparticles: Characterization, cytotoxicity evaluation and antibacterial activity. Applied Surface Science 463:66–74. https://doi.org/10.1016/j.apsusc.2018.08.203.

Sarkar MK, Vadivel V, Charan Raja MR &Mahapatra SK (2018) Potential anti-proliferative activity of AgNPs synthesized using *M. longifolia* in 4T1 cell line through ROS generation and cell membrane damage. Journal of Photochemistry and Photobiology B: Biology 186:160–168. https://doi.org/10.1016/j.jphotobiol.2018.07.014.

Satpathy S, Patra A, Ahirwar B &Delwar Hussain M (2018) Antioxidant and anticancer activities of green synthesized silver nanoparticles using aqueous extract of tubers of Pueraria tuberosa. Artificial Cells, Nanomedicine and Biotechnology 46:S71–S85. https://doi.org/10.1080/21691401.2018.1489265.

Sattari R, Khayati GR &Hoshyar R (2021) Biosynthesis of Silver–Silver Chloride Nanoparticles Using Fruit Extract of *Levisticum Officinale*: Characterization and Anticancer Activity Against MDA-MB-468 Cell Lines. Journal of Cluster Science 32:593–599. https://doi.org/10.1007/s10876-020-01818-3.

Shao Y, Wu C, Wu T, Yuan C, Chen S, Ding T &Hu Y (2018) Green synthesis of sodium alginate-silver nanoparticles and their antibacterial activity. International Journal of Biological Macromolecules 111:1281–1292. https://doi.org/10.1016/j.ijbiomac.2018.01.012.

SI A, Pal K, Kralj S, El-Sayyad GS, de Souza FG &Narayanan T (2020) Sustainable preparation of gold nanoparticles via green chemistry approach for biogenic applications. Materials Today Chemistry 17:100327. https://doi.org/10.1016/j.mtchem.2020.100327.

Singh A, Sharma B & Deswal R (2018) Green silver nanoparticles from novel Brassicaceae cultivars with enhanced antimicrobial potential than earlier reported Brassicaceae members. Journal of Trace Elements in Medicine and Biology 47:1–11. https://doi.org/10.1016/j.jtemb.2018.01.001.

Singh J, Mehta A, Rawat M & Basu S (2018) Green synthesis of silver nanoparticles using sun dried tulsi leaves and its catalytic application for 4-Nitrophenol reduction. Journal of Environmental Chemical Engineering 6:1468–1474. https://doi.org/10.1016/j.jece.2018.01.054.

Sunderam V, Thiyagarajan D, Lawrence AV, Mohammed SSS &Selvaraj A (2019) In-vitro antimicrobial and anticancer properties of green synthesized gold nanoparticles using *Anacardium occidentale* leaves extract. Saudi Journal of Biological Sciences 26:455–459. https://doi.org/10.1016/j.sjbs.2018.12.001.

Suriyakala G, Sathiyaraj S, Devanesan S, AlSalhi MS, Rajasekar A, Kannan Maruthamuthu M &Babujanarthanam R (2022) Phyto Synthesis of Silver Nanoparticles from *Jatropha integerrima Jacq.* Flower Extract and Their Possible Applications as Antibacterial and Antioxidant Agent. Saudi Journal of Biological Sciences 29:680–688. https://doi.org/10.1016/j.sjbs.2021.12.007.

Swamy MK, Akhtar MS, Mohanty SK &Sinniah UR (2015) Synthesis and characterization of silver nanoparticles using fruit extract of *Momordica cymbalaria* and assessment of their in vitro antimicrobial, antioxidant and cytotoxicity activities. Spectrochimica Acta - Part A: Molecular and Biomolecular Spectroscopy 151:939–944. https://doi.org/10.1016/j.saa.2015.07.009.

Thomas B, Vithiya BSM, Prasad TAA, Mohamed SB, Magdalane CM, Kaviyarasu K & Maaza M (2018) Antioxidant and Photocatalytic Activity of Aqueous Leaf Extract Mediated Green Synthesis of Silver Nanoparticles Using *Passiflora edulis flavicarpa*. Journal of Nanoscience and Nanotechnology 19:2640–2648. https://doi.org/10.1166/jnn.2019.16025.

Tosun F & Akyuz K Ç (2003) Anthraquinones and flavonoids from *Rheum ribes*. Ankara Universitesi Eczacilik Fakultesi Dergisi 32:31–35.

Umaz A, Koç A, Baran M F, Keskin C & Atalar M N (2019) Investigation of Antimicrobial Activity and Characterization, Synthesis of Silver Nanoparticles from *Hypericum triquetrifolium Turra* Plant. Iğdır Üniversitesi Fen Bilimleri Enstitüsü Dergisi 9:1467–1475. https://doi.org/10.21597/jist.533115.

Vastrad J (2016) Green Synthesis and Characterization of Silver Nanoparticles Using Leaf Extract of *Tridax Procumbens*. Asian Journal of Pharmaceutical and Research 7:44–48. https://doi.org/10.13005/ojc/320327.

Velmurugan P, Anbalagan K, Manosathyadevan M, Lee KJ, Cho, MinJung-Hee Park, Sae-Gang Oh K-SB, Oh B-T & Lee SM (2014) Green synthesis of silver and gold nanoparticles using *Zingiber officinale* root extract and antibacterial activity of silver nanoparticles against food pathogens. Bioprocess and Biosystems Engineering 37:1935–1943. https://doi.org/10.1007/s00449-014-1169-6.

Wang Y, Chinnathambi A, Nasif O & Alharbi SA (2021) Green synthesis and chemical characterization of a novel anti-human pancreatic cancer supplement by silver nanoparticles containing *Zingiber officinale* leaf aqueous extract. Arabian Journal of Chemistry 14:103081. https://doi.org/10.1016/j.arabjc.2021.103081.

Wongpreecha J, Polpanich D, Suteewong T, Kaewsaneha C & Tangboriboonrat P (2018a) One-pot, large-scale green synthesis of silver nanoparticles-chitosan with enhanced antibacterial activity and low cytotoxicity. Carbohydrate Polymers 199:641–648. https://doi.org/10.1016/j.carbpol.2018.07.039.

Wongpreecha J, Polpanich D, Suteewong T, Kaewsaneha C & Tangboriboonrat P (2018b) One-pot, large-scale green synthesis of silver nanoparticles-chitosan with enhanced antibacterial activity and low cytotoxicity. Carbohydrate Polymers 199:641–648. https://doi.org/10.1016/j.carbpol.2018.07.039.

Yixia Zh, Dapeng Y, Yifei K, Xiansong W & Omar Pandoli GG (2010) Synergetic Antibacterial Effects of Silver Nanoparticles *Aloe Vera* Prepared via a Green Method. Nano Biomedical Engineering 2:252–257. https://doi.org/10.5101/nbe.v2i4.p252-257.1.

Zein R, Alghoraibi I, Soukkarieh C, Salman A & Alahmad A (2020) *In-vitro* anticancer activity against Caco-2 cell line of colloidal nano silver synthesized using aqueous extract of *Eucalyptus Camaldulensis* leaves. Heliyon 6:e04594. https://doi.org/10.1016/j.heliyon.2020.e04594.